



IJVR

ISSN: 1728-1997 (Print)
ISSN: 2252-0589 (Online)

Vol. 21

No.4

Ser. No.73

2020

**IRANIAN
JOURNAL
OF
VETERINARY
RESEARCH**



Original Article

Sectional anatomic and tomographic study of the feline abdominal cavity for obtaining a three-dimensional vascular model

Rojo, D.^{1*}; Vázquez, J. M.¹; Sánchez, C.¹; Arencibia, A.²; García, M. I.³; Soler, M.⁴; Kilroy, D.⁵ and Ramírez, G.¹

¹Department of Anatomy and Comparative Pathological Anatomy, Veterinary Faculty, Campus of Espinardo, University of Murcia, 30100, Murcia, Spain; ²Department of Morphology, Veterinary Faculty, University of Las Palmas de Gran Canaria, Trasmontaña, Arucas, 35413 Las Palmas, Spain; ³Support Research Service, University of Murcia, 30100, Murcia, Spain; ⁴Department of Animal Medicine and Surgery, Veterinary Faculty, Campus of Espinardo, University of Murcia, 30100, Murcia, Spain; ⁵Division of Veterinary Science Centre, University College Dublin, School of Veterinary Medicine, Belfield, Dublin 4, Ireland

*Correspondence: D. Rojo, Graduated from Veterinary Faculty, Campus of Espinardo, University of Murcia, 30100, Murcia, Spain. E-mail: danielrojo@um.es

(Received 17 May 2020; revised version 16 Sept 2020; accepted 29 Sept 2020)

Abstract

Background: Unlike dogs, feline abdominal studies are rare. Note that anatomical studies in felines are scarce and almost unique using feline cadaver by means of sectional anatomy and computed tomography (CT) or magnetic resonance imaging (MRI). **Aims:** In this study, a non-pathological vascularization model of feline abdomen was conducted on three adult cats was using anatomical and diagnostic imaging techniques. **Methods:** A live pet cat and two cat cadavers were used in this study. Cat cadavers were injected with colored latex to show well-differentiated vascular structures and serial sections of cat abdomen were then provided. Computed tomography was performed by injecting an iodinated contrast medium through the cephalic vein of a live cat immediately before scanning. The CT images showed the arterial and venous vascular formations hyper-attenuated with two tomographic windows. The correlation between anatomical sections and their CTs was studied to identify vascular and visceral structures. **Results:** Hyper-attenuated vascular structures with the contrast medium were identified and marked along their path in the series of Dicom images with the Amira program. In this approach, sequentially and semiautomatically, vascular volumetric reconstruction was obtained without visceral formations. With the OsiriX program, volumetric reconstruction was automatic and maintained the fidelity of all visceral and vascular formations. **Conclusion:** We conclude that these improved prototypes could be used in veterinary clinics as normal vascular models and as a basis for obtaining future 3D models of vascular anomalies such as portosystemic shunts.

Key words: CT, Feline abdominal cavity, Sectional anatomy, Vascular model, Volumetric reconstruction

Introduction

A recent increased number of feline patients in veterinary clinics and more common use of diagnostic imaging techniques for detection of vascular pathologies of a feline abdomen has focused our interest in this anatomical region and species. However, most studies have been carried out on canine abdomen using computed tomography (CT) and radiology (RX). Crawford, Manley and Adams (2003) bring to light the scarce and low-quality work on the anatomy of the canine abdomen using CT. Teixeira *et al.* (2007) made a study of the normal anatomy of the canine abdomen in four mature crossbreed dogs using helical computed tomographic images with iodinated contrast medium whereas Smallwood and George (1992) studied both thorax and cranial canine abdomen by computerized tomography.

Other studies have focused on analyzing the irrigation of the abdomen using tomography. Dennis

(2005) tried to establish whether location of celiac and cranial mesenteric arteries was sufficiently consistent to be used as anatomical landmarks. Also, CT and magnetic resonance imaging (MRI) were used to study congenital vascular abnormalities by Boffman and Thrall (2006), Frank *et al.* (2003) and Oui *et al.* (2013) reporting the first persistent left cranial vena cava and multiple abdominal malformations in a dog. Schwarz *et al.* (2009) described features of segmental caudal vena cava aplasia and associated vascular anomalies by CT and magnetic resonance in dogs. In addition, Zwingenberger *et al.* (2005) explained the use of a dual phase computed tomographic angiography technique to diagnose arterioportal fistulae in four dogs.

In other CT studies, intervertebral lumbosacral joints (Axlund and Hudson, 2003), a genitourinary excretory system through intravenously urography (Rozear and Tidwell, 2003), adrenal glands (Bertolini *et al.*, 2006), and canine pancreas (Cáceres *et al.*, 2006) have been analyzed.

Unlike dogs, feline abdominal studies are rare. A cadaver study by means of sectional anatomy and CT was carried out by Samii *et al.* (1998). Other CT studies used live cats (Shojaei *et al.*, 2006), and iodinated contrast medium (Samii *et al.*, 1998). Head *et al.* (2003) tested the viability and usefulness of CT for clinical evaluation of pancreas in six normal cats. According to a study of Bouma *et al.* (2003), CT scans of feline renal vascular anatomy are feasible, and reconstruction techniques provided excellent anatomical vascular detail.

The studies of magnetic resonance imaging in cats produced high quality images as sectional anatomy was correlated with magnetic resonance images (Samii *et al.*, 1999). Later, Newell *et al.* (2016) obtained magnetic resonance images of the cranial and middle abdomen with a contrast medium in 15 clinically normal cats.

This literature review prompted us to undertake an anatomically detailed study of the feline abdominal cavity using contrast CT and anatomical sections with vascular repletion in the cadavers, in order to evaluate a correlation between the CT images with the anatomical sections. The second goal of this study was to obtain a vascular prototype printed in 3D that helps veterinary clinicians to better identify the feline abdominal anatomy, to improve the diagnosis and treatment of vascular pathologies of the feline abdomen, and to promote the teaching quality of the normal anatomy.

Materials and Methods

Animals

Three entire, two crossbreed cat cadavers (*Felis silvestris catus*, L.), males, 3-4 years old and about 3.5-4 kg belonging to Zoonoses Service of Murcia were used to obtain gross sections of the abdomen. A live 3 years old male domestic cat (3 kg) was also used for CT angiography study. Written informed consent was obtained from the owner of the cat used for this research. Both cadavers obtained from the Public Health Service were humanely euthanized for causes unrelated to this study. The Public Health Service cats had a moderately filled stomach but the live pet was off feed because it was anesthetized for CT angiography. Verbal consent of pet owners and experimental procedures were supervised and approved by animal care and ethics committee of the University of Las Palmas de Gran Canaria, Spain (MV-2015/08).

Radiology and computed tomography techniques

The live pet cat was used for a radiological and CT study of the abdomen. The study was made under the supervision of the Ethics Commission of the University of Las Palmas de Gran Canaria (MV-2015/08). The cat was pre-anaesthetized with dexmedetomidine (Dexdomitor, Orion Farma) (40 mcg/kg) and Butorphanol (Thorphasol, Esteve) (0.4 mg/kg) intramuscular (IM). Twenty-five min after premedication a 20-gauge catheter was placed in the right cephalic vein and flushed with saline solution (8 ml/kg). Anaesthesia

was induced with propofol (Propofol-Lipuro 1%, Braun) 4 mg/kg. Anaesthesia was maintained with a mixture of 1.5% isoflurane (Forane, Abbott) in 100% oxygen, using a semi-closed circle rebreathing circuit. Mechanical ventilation was performed throughout the scan. The cat was examined in sternal recumbency using a 16-detector helical scanner (CT HiSpeed Siemens SOM5). After the initial examination, only one CT angiography was performed using non-ionic contrast medium iohexol (Omnitrac, Schering) at 800 mg/kg and at 3 ml/s into cephalic vein catheter by angiographic injector (A-60, Nemoto) near body temperature (38.5°C). The CT scan started at the level of diaphragmatic dome and the end point of the scan was at the level of the pelvic cavity. Data acquisition and contrast medium injection were started simultaneously and arterial and venous phases were taken into account.

Technical parameters were as follows: tube voltage (120 kV), tube current (120 mAs), tube rotation time (1 s/rotation), helical scan mode, collimator pitch of 1.5, 3 mm (o: 1.2 mm) slice thickness and reconstructions interval with 50% overlap. The display field of view was 25 cm and image matrix 512 × 512. On the CT workstation, images were obtained with soft tissue and bone algorithms and reformatted in sagittal and dorsal planes, maximum intensity projection (MIP) and volume rendering (VR). Images were reviewed in a Picture Archiving and Communication System (PACS) workstation (AGFA Healthcare CR10-X digital processor) in soft tissue (WW=400, WL=40) and mediastinum-vascular windows (WW=350, WL=40). The Dicom files generated by the CT scanner were analyzed with the OsiriX and Amira programs. Through the application of different post-processing algorithms, images of MIP, surface and volumetric reconstructions were subsequently obtained, which resulted in a 3D printing of the structures of the feline abdomen through the program Slicer 3.0. The cost of performing 3D printing was about 75 to 100 € per model, depending on the size scale.

Anatomical evaluation

The cat cadavers were transported to the dissection room and vascular pumping with 2% saline solution was carried out. Subsequently, these specimens were injected via the common carotid artery and external jugular vein with red and blue latex, respectively. To obtain the anatomical sections, the specimens were initially frozen at -20°C. Abdominal blocks were prepared and then frozen at -80°C for at least 48 h before sectioning with a band saw machine (Anatomical Lab., Department of Anatomy and Embryology, University of Murcia, Spain). About 200 cross sections were obtained with 0.7-1 cm thickness. Sections were then photographed at both their cranial and caudal aspects to evaluate their correlation with the CT images.

Results

The radiographic image was divided into three

regions to establish more complete analysis of the vascular structures at the level of the cranial, middle and caudal abdomen.

Figure 1 shows a lateral radiograph with lines representing the location of each anatomical transverse cross section and CT image.

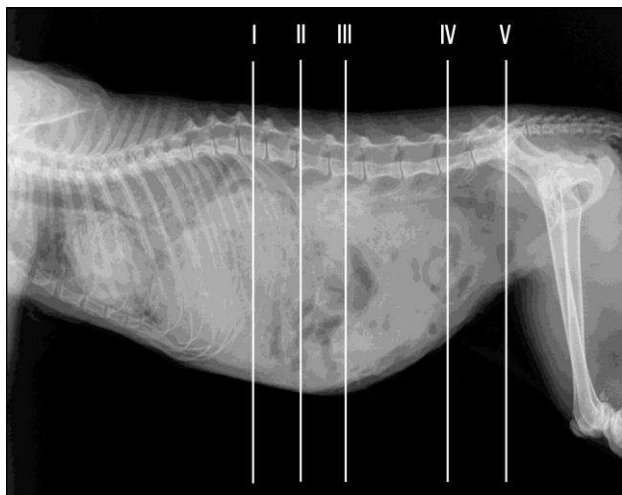


Fig. 1: Approximated level of section of cat abdomen. Lines represent the location of each transverse anatomical section and CT image (levels I-V)

Anatomical sections and CT angiography

Cranial abdomen

The fundus of the stomach, the hepatic (caudate, quadrate, right and left) lobes, and the gallbladder were observed. Injected arteries and veins were clearly differentiated in anatomical sections and could be correlated in tomographic images as they were hyper-attenuated by contrast. The right testicular artery was clearly seen but the left testicular artery was not visualized in the CT study as the contrast medium did not fill that artery, and in the anatomical sections, neither testicular artery was observed. In addition, vascular structures such as the thoracic aorta, caudal vena cava, and the portal vein (bloodless) were clearly seen in the anatomical sections. The hepatic artery branches were identified as very small red branches in the hepatic porta, but the hepatic veins branches and portal vein branches (blue) were not distinguished among them. At this level, it was still possible to appreciate the right and left caudal lung lobes.

The stomach and colon walls showed a hyper-attenuated appearance with respect to the content that was visualized hypo-attenuated with the mediastinum vascular window. The liver was hypo-attenuated on CT with mediastinum vascular and soft tissue windows with respect to renal imaging. The use of intravenous contrast agents allowed the study of the hepatic veins, with enhanced hyper-attenuated images. The pancreas was identified as a hypo-attenuated structure in relation to the spleen and liver; after the introduction of the contrast medium, it was easier to identify. The liver showed a low attenuation with the mediastinum vascular window with respect to the soft tissue window, which allowed better

visualization of the hepatic lobes and interlobar fissure. The gallbladder was hypo-attenuated in the vascular mediastinum window and slightly hypo-attenuated in the soft tissue window compared with the liver. Bile ducts were not appreciated either in anatomical sections or in CT scans. The contrast medium allowed the identification of the hyper-attenuated aorta, caudal vena cava, and portal veins in both windows. The portal veins were very small and hyper-attenuated and it was not possible to distinguish their branches from the branches of the hepatic veins (Figs. 2A, B and C).

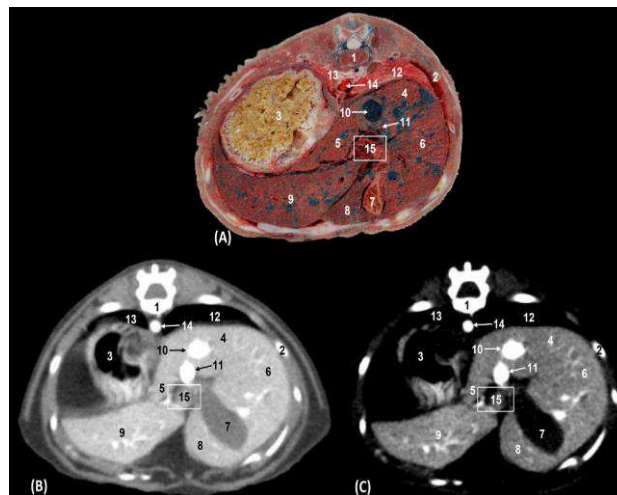


Fig. 2: Transverse sections of the cranial abdomen at the level of the thirteenth thoracic vertebra (level D). (A) Anatomical section, (B) Soft tissue window CT image, and (C) Mediastinum-vascular window CT image. Caudal views. 1: Thoracic vertebra: body, 2: Rib: body, 3: Stomach: body, 4: Liver: caudate lobe; caudate process, 5: Liver: Caudate lobe; papillary process, 6: Liver: right lateral lobe, 7: In liver gallbladder: quadrate lobe, 8: Liver: left medial lobe, 9: Liver: left lateral lobe, 10: Caudal vena cava, 11: Portal vein (in A bloodless), 12 = Right lung: caudal lobe, 13: Left lung: caudal lobe, 14: Thoracic aorta, and 15: Porta of liver

We could distinguish between the descending duodenum, the transverse colon and the jejunal coils, and both the body and the pyloric antrum of the stomach. The walls of the stomach, colon, duodenum, and pancreas were hyper-attenuated in both types of windows. The contents of the stomach, duodenum, and colon were observed as slightly hyper-attenuated in soft tissue and hypo-attenuated in the mediastinum vascular window. The kidneys and the spleen appeared clearly in anatomical sections and were hypo-attenuated in both CT windows. We observed, ventral to the vertebral column, the abdominal aorta, and to the right side of the abdomen, the caudal vena cava and underlying it, the cranial mesenteric artery and vein. Branches of the splenic artery and vein were located in anatomical sections and both CT windows (Figs. 3A, B and C).

Middle abdomen

The descending duodenum, the ascending colon, the jejunal coils and the pancreatic right lobe were observed, as well as both kidneys, spleen, mesentery, and the

greater omentum. The vascular structures identified at this level were the caudal vena cava, right renal artery and vein, left renal vein, splenic artery, and vein (Figs. 4A, B and C).

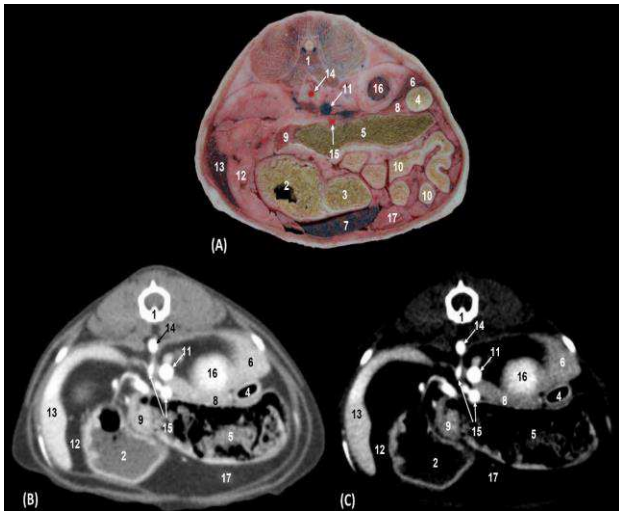


Fig. 3: Transverse sections of the cranial abdomen at the level of the second lumbar vertebra and cranial pole of right kidney (level II). (A) Anatomical section, (B) Soft tissue window CT image, and (C) Mediastinum-vascular window CT image. Caudal view. 1: Lumbar vertebra: body, 2: Stomach: body, 3: Stomach: pylorus, 4: Descending duodenum, 5: Transverse colon, 6: Liver: caudate lobe; caudate process, 7: Liver: left lateral lobe, 8: Pancreas: right lobe, 9: Pancreas: left lobe, 10: Jejunal coils, 11: Caudal vena cava, 12: Gastrosplenic ligament, 13: Spleen, 14: Abdominal aorta, 15: Cranial mesenteric artery, 16: Cranial pole of right kidney, and 17: Greater omentum

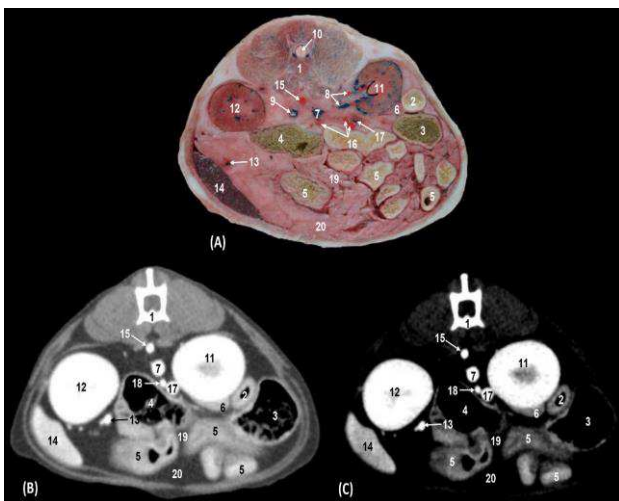


Fig. 4: Transverse section of the middle abdomen between left and right kidneys (level III). (A) Anatomical section, (B) Soft tissue window CT image, and (C) Mediastinum vascular window CT image. Caudal views. 1: Lumbar vertebra: body, 2: Descending duodenum, 3: Ascending colon, 4: Descending colon, 5: Jejunal coils, 6: Pancreas: right lobe, 7: Caudal vena cava, 8: Right kidney artery and vein, 9: Left kidney vein, 10: Spinal cord, 11: Right kidney, 12: Left kidney, 13: Splenic artery and vein, 14: Spleen, 15: Abdominal aorta, 16: Cranial mesenteric artery: branches, 17: Portal vein, 18: Cranial mesenteric vein, 19: Mesentery, and 20: Greater omentum

Caudal abdomen

The descending and ascending duodenum, the ascending and descending colon, the jejunal coils, pancreatic right lobe, spleen, and ascending duodenum were observed as well as vascular structures such as the caudal vena cava, the splenic artery and splenic vein and abdominal aorta. Jejunal vessels (branches of the cranial mesenteric artery and vein) were perfectly delineated in both anatomical sections and both CT windows. The splenic vessels allowed the identification of the pancreas with both types of windows (Figs. 5A, B and C).

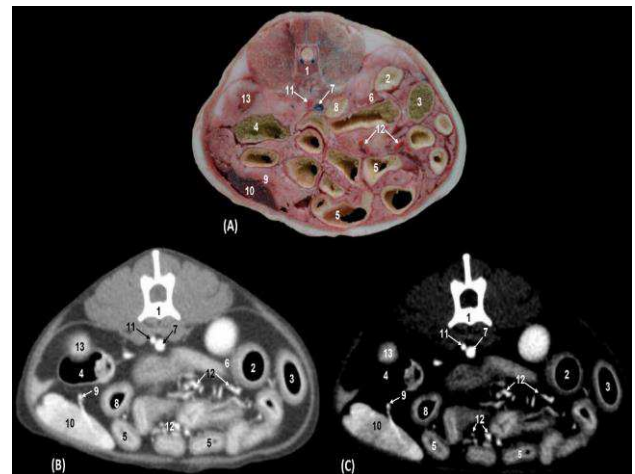


Fig. 5: Transverse section of the caudal abdomen at level of the sixth lumbar vertebra (level IV). (A) Anatomical section, (B) Soft tissue window CT image, and (C) Mediastinum vascular window CT image. Caudal views. 1: Lumbar vertebra: body, 2: Descending duodenum, 3: Ascending colon, 4: Descending colon, 5: Jejunal coils, 6: Pancreas: right lobe, 7: Caudal vena cava, 8: Ascending duodenum, 9: Splenic artery and vein, 10: Spleen, 11: Abdominal aorta, 12: Branches of the cranial mesenteric artery, and 13: Left kidney

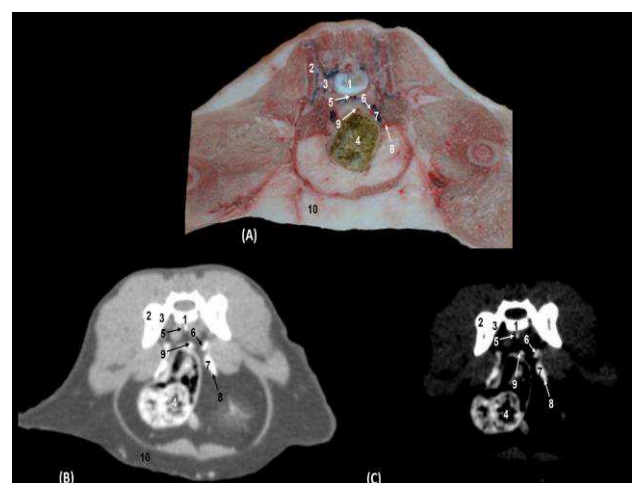


Fig. 6: Transverse section of the caudal abdomen at the level of the sacroiliac joint (first sacral vertebra) (Level V). (A) Anatomical section, (B) CT with soft tissue window CT image, and (C) Mediastinum vascular window CT image. Caudal views. 1: Sacrum: body, 2: Sacrum: wing, 3: Ilium: wing, 4: Descending colon, 5: Median sacral artery and vein, 6: Internal iliac artery, 7: Common iliac vein, 8: External iliac artery, 9: Cranial rectal artery, and 10: Abdominal fat

The descending portion of the colon and vascular structures with colored latex was observed. In CT scans with both window types, vascular structures such as the median sacral artery and vein, internal iliac artery, common iliac vein, external iliac artery, and cranial rectal artery were highly attenuated (Figs. 6A, B and C).

Volumetric reconstructions and 3D printing

In volumetric reconstruction using OsiriX and Amira, and in 3D printed images of the left aspect of the abdominal cavity, the liver, the spleen, and both kidneys were clearly observed. In OsiriX images jejunal coils and the descending colon were well appreciated but not the right kidney. However, vascular structures such as the abdominal aorta, caudal vena cava, left testicular artery and external iliac artery were clearly recognized. The hepatic veins and branches of the cranial mesenteric vein were seen both in Amira and in 3D printed images. Visualization of the portal vein was possible only in the Amira images. The common iliac vein was not well distinguished in the OsiriX images, but it was clearly observed in the Amira and 3D prints (Figs. 7A, B and C). The liver and both kidneys were clearly observed on the right side of the abdominal cavity in the volumetric reconstruction OsiriX and Amira, and 3D printed images; however, while jejunal coils and the descending colon were visualized in the OsiriX image, the right kidney was not identified. The spleen was only seen in

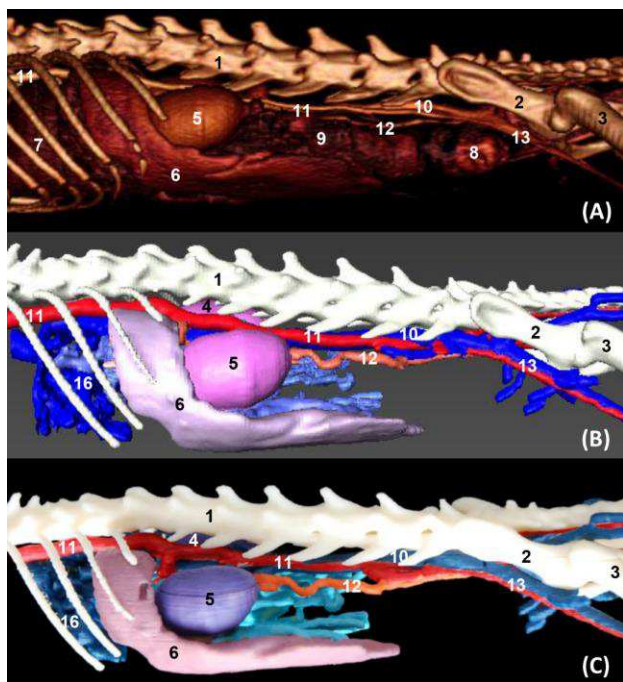


Fig. 7: Volumetric reconstruction (volume rendering) of the abdominal and pelvic cavities together with the bones of the spine, ribs, and hip joint performed with the (A) OsiriX program, (B) Amira for Fei Systems, and (C) Colored three-dimensional printing. Left side view. 1: Lumbar vertebrae, 2: Ilium: body, 3: Femur, 4: Right kidney, 5: Left kidney, 6: Spleen, 7: Liver, 8: Descending colon, 9: Intestine: coils, 10: Caudal vena cava, 11: Abdominal aorta, 12: Left testicular artery, and 13: External iliac artery and vein

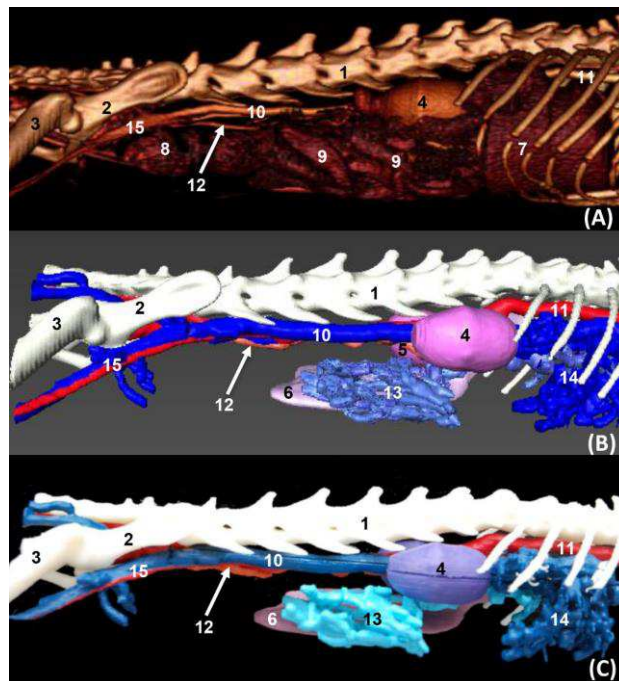


Fig. 8: Volumetric reconstruction (volume rendering) of the abdominal and pelvic cavities together with the bones of the spine, ribs, and hip joint performed with the OsiriX (A), program, Amira for Fei Systems (B), and three-dimensional impression (C). Right side view. 1: Lumbar vertebrae, 2: Ilium: body, 3: Femur, 4: Right kidney, 5: Left kidney, 6: Spleen, 7: Liver, 8: Descending colon, 9: Intestine: coils, 10: Caudal vena cava, 11: Abdominal aorta, 12: Left testicular artery, 13: Jejunal veins, 14: Hepatic veins, and 15: External iliac artery and vein

Amira and 3D printed images. Regarding vascular structures, the caudal vena cava, common iliac vein and external iliac artery together with the left testicular artery were clearly observed. Finally, it was noted that the branches of the cranial mesenteric, hepatic and portal veins were seen only in Amira and 3D printing images (Figs. 8A, B and C).

In the images of volumetric reconstruction (OsiriX and Amira) and 3D printing in ventral vision, the abdominal cavity clearly showed the liver, both kidneys, stomach, spleen, jejunal coils, descending colon, and rectum in the OsiriX image. The spleen and kidneys were seen in Amira and 3D printed images. The caudal vena cava, the common iliac vein, and the external iliac artery along with the left testicular artery were well appreciated. The branches of the cranial mesenteric vein between the jejunal coils were observed in the OsiriX image, while the Amira and 3D printed images clearly showed the tributaries of the portal vein (cranial mesenteric, gastroduodenal, and splenic veins) and hepatic veins (Figs. 9A, B and C).

In volumetric reconstruction using OsiriX and Amira, and 3D printed images (dorsal view), the abdominal cavity clearly showed the liver, stomach, both kidneys, stomach, spleen, jejunal coils, descending colon, and rectum in the OsiriX image. The spleen, kidneys, and hepatic veins were seen in Amira and 3D printed images. Renal arteries and renal veins, the left testicular artery,

branches of the cranial mesenteric vein, and splenic vessels were observed in all images. The hepatic veins were seen only in Amira and 3D printed images (Figs. 10A, B and C).

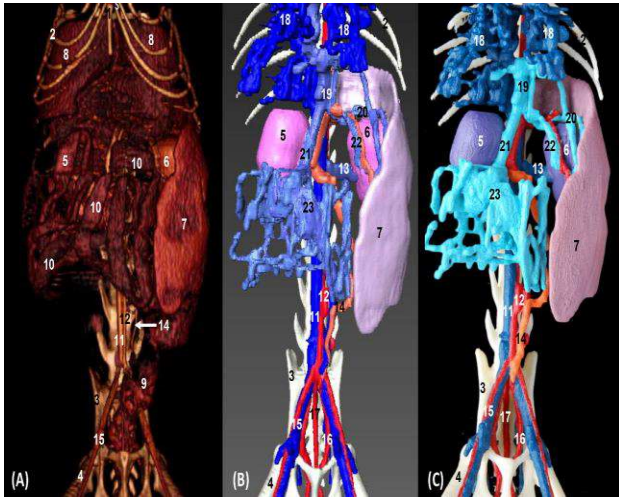


Fig. 9: Volumetric reconstruction (volume rendering) of the abdominal and pelvic cavities together with the bones of the spine, ribs, and hip joint performed with the (A) OsiriX program, (B) Amira for Fei Systems, and (C) three-dimensional impression (ventral vision). 1: Sternum; xiphoid process, 2: Ribs, 3: Ilium, 4: Femur, 5: Right kidney, 6: Left kidney, 7: Spleen, 8: Liver, 9: Descending colon, 10: Intestine: coils, 11: Caudal vena cava, 12: Abdominal aorta, 13: Left renal vein, 14: Left testicular artery, 15: External iliac artery and vein, 16: Internal iliac artery, 17: Median sacral artery, 18: Hepatic veins, 19: Portal vein, 20: Splenic arteries and veins, 21: Cranial Mesenteric vein, 22: Gastroduodenal vein, and 23: Jejunal veins

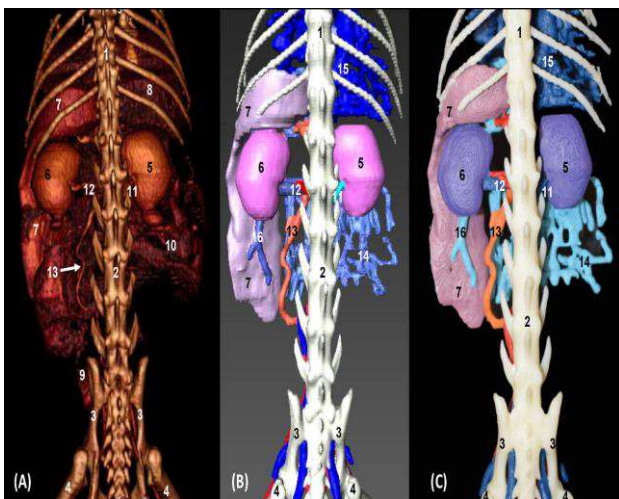


Fig. 10: Volumetric reconstruction (volume rendering) of the abdominal and pelvic cavities together with the bones of the spine, ribs, and hip joint performed with the (A) OsiriX program, (B) Amira for Fei Systems, and (C) Three-dimensional impression (dorsal view). 1: Thoracic vertebra, 2: Lumbar vertebrae, 3: Ilium, 4: Femur, 5: Right kidney, 6: Left kidney, 7: Spleen, 8: Liver, 9: Descending colon, 10: Intestine: coils, 11: Right renal artery and vein, 12: Left renal artery and vein, 13: Left testicular artery, 14: Jejunal veins, 15: Hepatic veins, and 16: Splenic vein

Discussion

For the interpretation of anatomical sections, it is necessary to consider variations in the size, shape and anatomical relations of the abdominal organs, which partly depend on their degree of fullness. The abdominal organs and structures were interpreted, identified and differentiated according to the level of the section. To facilitate the identification of different anatomical structures, especially the vascular ones, bone (vertebral bodies, ribs), and visceral references (hepatic lobes, kidney, stomach and duodenum) have been used to identify the continuity of certain structures such as the caudal vena cava, aorta, portal vein and the cranial mesenteric artery and vein.

All the visceral structures were easily identified by means of CT; however, to recognize vascular structures it was necessary to follow each vessel using the image sequence of the Amira program. The study of CT with contrast media performed on the canine abdomen by Teixeira *et al.* (2007) did not employ anatomical sections, nevertheless, vascular formations were observed very clearly as they were hyper-attenuated. In addition, the hepatic veins were seen with both types of windows and in our anatomical sections were distinguished by being dyed with blue latex. The images of the visceral branches of the abdominal aorta of the middle and caudal abdomen observed in our study mostly coincided with those observed in the studies in the dog. Similarly to Teixeira *et al.* (2007), we could appreciate all the visceral branches of the abdominal aorta, except the testicular and the caudal mesenteric vessels. On the other hand, we observed a description of the intrahepatic bile ducts in the dog, which was not detected in our feline study, nor a common hepatic duct; this found is in compliance with Schaller (1992). Few publications have correlated CT with anatomical sections in the canine abdomen, but Smallwood and George (1992) analyzed topography of the ureters, urinary bladder, ovary and uterus to the internal and external iliac artery, but there were no references to the veins nor was there vascular filling with latex in the anatomic sections, so this study did not provide information to facilitate the identification of vasculature. These authors similarly described the main viscera and the larger blood vessels such as the abdominal aorta, portal vein, and caudal vena cava. However, their study did not describe any visceral branch of the abdominal aorta or tributaries of the caudal vena cava to aid the identification of these formations in the feline abdomen. Studies of Zwingenberger *et al.* (2005) about the portal and hepatic vascular system of the dog by CT angiography or CT of dual phase, helped to corroborate our identification of the hepatic veins, cranial mesenteric, gastroduodenal, splenic and portal veins. However, we were not able to identify the caudal mesenteric vein or the branching of the intrahepatic portal vein into the different hepatic lobes as described in their work. In our study, we identified two branches of the splenic vein draining into the caudal vena cava. Bertolini *et al.* (2006) emphasized the usefulness of

three-dimensional (3D) multislice CT angiography with MIP and volume rendering (VR) in dogs with portosystemic shunts, describing the main vessels (abdominal aorta, caudal vena cava, portal vein and the anomalous vessel: porto-caval or porto-azygous). This manuscript allowed us to corroborate the arrangement of our vascular formations, except for the branches derived from the main trunks. We believe that this work will provide valuable information for the 3D study of vascularization, aiding the study of vascular anomalies.

Studies carried out in the abdomen of the cat by Samii *et al.* (1998) which combines sectional anatomy and CT with contrast media, and Samii *et al.* (1999) using MRI, helped us to study some large vessels such as the abdominal aorta, caudal vena cava and portal vein. The CT images of the feline abdomen by Shojaei *et al.* (2006) allowed us to localize and analyze the images of the abdominal aorta, the portal vein and the caudal vena cava. We found additional information in identifying the main structures of the cranial abdomen of the cat in the work of Newell *et al.* (2016) employing MRI. Our study did not locate two branches in the right and left renal vein, nor the left renal accessory artery described in the angiographic CT study of the feline kidney by Bouma *et al.* (2003). MRI study of Dennis (2005), performed on 95 dogs and 5 cats, showed the position of the celiac and cranial mesenteric arteries, but it did not show any MRI image in the cat, not comparable with our images. Studies of MRI with contrast medium of portosystemic shunts were exerted in cats by Scavelli *et al.* (1986) and in dogs by Frank *et al.* (2003) allowed us to appreciate the normal vascular pattern. Both authors and Schwarz *et al.* (2009) in the study of canine shunts through the use of CT angiography and MRI, and Oui *et al.* (2013) describing multiple anomalies of the caudal vena cava in a dog using CT, agreed and indicated the importance of obtaining volumetric reconstructions to clarify these vascular anomalies and encourage the need to perform a study in a normal vascular model.

A radiographic study with contrast medium or arteriography performed by Kneller *et al.* (1972) in cats supported our study's description of the disposition of the visceral branches of the abdominal aorta and its similar topography to the dog.

CT angiographic study conducted by Grabherr *et al.* (2005) in three cadaver specimens (two dogs and a cat) using a fluid of diesel oil and a lipophilic contrast media, produced a large 3D volumetric reconstruction but with poor detail in its interpretation; however, it is a good study of the disposition of vascular formations in carnivores, which helped us in producing a 3D model. In order to carry out our tomographic study of contrast and 3D reconstruction, we relied on the scanner settings used in the study of the human ear by Fatterpekar *et al.* (2006) and we also used this research as a reference to perform the 3D printing. Regarding the reconstruction, we concur with Lauridsen *et al.* (2018) in the acquisition of the image made with a 16 detector CT scanner. The treatment of the images was done with Amira, we also used the program OSIRIX, which allowed us to compare

the results of both programs. To prepare 3D printing we generated a Standard Triangle Language (STL) file as in Hespel *et al.* (2014) and Lauridsen *et al.* (2018).

The correlation between the images of OsiriX, Amira, and 3D printing is a good example of what a normal 3D model of the feline abdomen vascularization can help veterinary clinicians. In future, 3D printed models of portosystemic shunts should be created to help clinicians understand these anomalies for more surgical resolution and could contribute to the teaching of normal anatomy.

Acknowledgements

Authors wish to thank M. O. Hernandez who performed the 3D painting. Computed tomography acquisitions were financed by Department of Anatomy and Comparative Pathological Anatomy, Veterinary Faculty, University of Murcia, Spain.

The authors received no financial support for the research, authorship or publication of this article. Computed tomography acquisitions were financed by Department of Anatomy and Comparative Pathological Anatomy, Veterinary Faculty, University of Murcia, Spain.

Conflict of interest

The authors of this manuscript have no conflict of interest to declare.

References

- Axlund, T and Hudson, J (2003). Computed tomography of the normal lumbosacral intervertebral disc in 22 dogs. *Vet. Radiol. Ultrasound.*, 44: 630-634.
- Bertolini, G; Furlanello, T; De Lorenzi, D and Caldin, M (2006). Computed tomographic quantification of canine adrenal gland volume and attenuation. *Vet. Radiol. Ultrasound.*, 47: 444-448.
- Boffman, P and Thrall, D (2006). Magnetic resonance imaging findings in a dog with caudal aortic thromboembolism and ischemic myopathy. *Vet. Radiol. Ultrasound.*, 47: 334-338.
- Bouma, JL; Aronson, LR; Keith, DG and Mark Saunders, H (2003). Use of computed tomography renal angiography for screening feline renal transplant donors. *Vet. Radiol. Ultrasound.*, 44: 636-641.
- Cáceres, AV; Zwingenberger, AL; Hardam, E; Lucena, JM and Schwarz, T (2006). Helical computed tomographic angiography of the normal canine pancreas. *Vet. Radiol. Ultrasound.*, 47: 270-278.
- Crawford, J; Manley, P and Adams, W (2003). Comparison of computed tomography, tangential view radiography, and conventional radiography in evaluation of canine pelvic trauma. *Vet. Radiol. Ultrasound.*, 44: 619-628.
- Dennis, R (2005). Assessment of location of the celiac and cranial mesenteric arteries relative to the thoracolumbar spine using magnetic resonance imaging. *Vet. Radiol. Ultrasound.*, 46: 388-390.
- Fatterpekar, GM; Doshi, A and Delman, BN (2006). *CT of the temporal bone anatomy and pathology. Clinical case*

- studies in the third dimension*. Vol. 2, San Mateo, CA, USA, TeraRecon Inc., PP: 187-208.
- Frank, P; Mahaffey, M; Egger, C and Cornell, KK** (2003). Helical computed tomographic photography in ten normal dogs and ten dogs with portosystemic shunt. *Vet. Radiol. Ultrasound.*, 44: 392-400.
- Grabherr, S; Djonov, V; Friess, A; Thali, MJ; Ranner, G; Vock, P and Dirnhofner, R** (2005). Postmortem angiography after vascular perfusion with diesel oil and a lipophilic contrast agent. *AJR Am.*, 187: 516-523.
- Head, LL; Daniel, GB; Tobias, K; Morandi, F; Denovo, RC and Donnell, R** (2003). Evaluation of the feline pancreas using tomography and radiolabeled leucocytes. *Vet. Radiol. Ultrasound.*, 44: 420-428.
- Hespe, AM; Wilhite, R and Hudson, J** (2014). Invited review-applications for 3D printers in veterinary medicine. *Vet. Radiol. Ultrasound.*, 55:347-358.
- Kneller, SK; Lewis, RE and Barrett, RB** (1972). Arteriographic anatomy of the feline abdomen. *J. Vet. Res.*, 33: 2111-2119.
- Lauridsen, H; Hansen, K; Nørgård, MØ; Wang, T and Pedersen, M** (2018). From tissue to silicon to plastic: three-dimensional printing in comparative anatomy and physiology. *R. Soc. Open Sci.*, 3: 150643.
- Nielsen, T; Lindström, L; Ingman, J; Uhlhorn, M and Hansson, K** (2016). High-frequency ultrasound of Peyer's patches in the small intestine of young cats. *J. Feline Med. Surg.*, 18: 303-309.
- Oui, H; Kim, J; Bae, Y; Oh, J; Park, S; Lee, G; HOON, J and Choi, J** (2013). Computed tomography angiography of situs inversus, portosystemic shunt and multiple vena cava anomalies in a dog. *J. Vet. Med. Sci.*, 75: 1525-1528.
- Rozear, L and Tidwell, AS** (2003). Evaluation of the ureter and ureterovesicular junction using helical computed tomographic excretory urography in healthy dogs. *Vet. Radiol. Ultrasound.*, 44: 155-164.
- Samii, VF; Biller, DS and Koblik, PD** (1998). Normal cross-sectional anatomy of the feline thorax and abdomen: comparison of computed tomography and cadaver anatomy. *Vet. Radiol. Ultrasound.*, 39: 504-511.
- Samii, VF; Biller, DS and Koblik, PD** (1999). Magnetic resonance imaging of the normal feline abdomen: an anatomic reference. *Vet. Radiol. Ultrasound.*, 40: 486-490.
- Scavelli, TD; Hornbuckle, WE; Roth, L; Rendano Jr, VT; De Lahunta, A; Center, SA; French, TW and Zimmer, JF** (1986). Portosystemic shunts in cats: seven cases (1976-1984). *J. Am. Vet. Med. A.*, 189: 317-325.
- Schaller, O** (1992). *Illustrated veterinary anatomical nomenclature*. 3rd Edn., Stuttgart, Ferdinand Enke Verlag. PP: 1-614.
- Schwarz, T; Rossi, F; Wray, JD; Åblad, B; Beal, MW Kinns, J; Seiler, GS; Dennis, R; McConnell, JF and Costello, M** (2009). Computed tomographic and magnetic resonance imaging features of canine segmental caudal vena cava aplasia. *J. Small Anim. Pract.*, 50: 341-349.
- Shojaei, B; Vajhi, AR; Rostami, A; Molaei, MM; Arashian, I and Hashemnia, S** (2006). Computed tomographic anatomy of the abdominal region of cat. *Iran. J. Vet. Res.*, 7: 45-52.
- Smallwood, JE and George, TF** (1992). Anatomic atlas for computed tomography in the mesocephalic dog: caudal abdomen and pelvis. *Vet. Radiol. Ultrasound.*, 33: 143-167.
- Teixeira, M; Gil, F; Vazquez, JM; Cardoso, L; Arencibia, A; Ramirez-Zarzosa, G and Agut, A** (2007). Helical computed tomography of the canine abdomen. *Vet. J.*, 174: 133-138.
- Zwingerberger, AL; McLear, C and Weisse, C** (2005). Diagnosis of arterioportal fistulae in four dogs using computed tomographic angiography. *Vet. J.*, 46: 472-477.